Tuesday, October 14, 2003
Afternoon Session I
GEOLOGY OF THE MARTIAN SOUTH POLAR LAYERED DEPOSITS *(Continued)*
1:30 p.m. Victoria Room

Kolb E. J. * Tanaka K. L.
Detailed Geologic Analysis of Part of the South Polar Layered Deposits, Planum Australe, Mars **[#8116]**

van Gasselt S. * Jaumann R.
Chasma Australe, Mars: Formation by Successive Headward Thermo-Erosional Collapses **[#8098]**

GENERAL DISCUSSION

GEOLOGY OF THE MARTIAN NORTH POLAR LAYERED DEPOSITS

Fishbaugh K. E. * Head J. W. III [INVITED]
Amazonian Geologic History of the North Polar Cap of Mars: Stratigraphy, Melting, and Retreat **[#8050]**

Payne M. C. * Farmer J. D.
Using Mars Orbiter Laser Altimeter Data to Detect Subglacial Features at the Residual North Polar Ice Cap **[#8002]**

Ng F. S. L. * Zuber M. T.
Albedo Feedback in the Patterning Mechanisms of Martian Polar Caps **[#8061]**

3:30 – 3:45 p.m. BREAK

DETAILED GEOLOGIC ANALYSIS OF PART OF THE SOUTH POLAR LAYERED DEPOSITS, PLANUM AUSTRALE, MARS.
E.J. Kolb[1] and K.L. Tanaka[2], [1]Arizona State University, Dept. of Geological Sciences, Tempe, AZ 85287, eric.kolb@asu.edu, [2]Astrogeology Team, U.S. Geological Survey, 2255 N. Gemini Dr., Flagstaff, AZ 86001, ktanaka@usgs.gov.

Introduction. We have begun geologic mapping of the martian south polar layered deposits (SPLD) as part of a project to map PLD at both poles at 1:1,500,000 scale. In this abstract, we present preliminary geologic mapping results of SPLD exposed in a trough system east of and adjacent to Chasma Australe within Planum Australe (Fig. 1). Our mapping has allowed us to address outstanding SPLD-related issues including: SPLD bedding characterization, relative timing and modes of trough emplacement, and the formation of secondary features such as the north-trending ridged-and-grooved ("wire brush") terrain and the sinuous, generally east-trending ridges ("snakes"). The major goals of the mapping project consist of: (1) Construction of stratigraphic sections of the PLD, including topographic analysis of prominent layers and layer sequences and investigation of intra- and interpolar stratigraphic and topographic variations in the PLD and residual ice caps, (2) detection and interpretation of structural deformation in the PLD, (3) description and interpretation of the erosional history of the PLD. Geologic mapping of the PLD is being performed using a GIS-integrated, multi-dataset approach consisting of current and to-be-released data products including MOLA topography, MOC NA images and THEMIS VIS and IR datasets.

Here, we discuss the geology of the SPLD within a broad trough whose floor dips gently from near the center of the SPLD down toward the margin of Planum Australe. This north-trending, radially orientated trough portrays some diverse and enigmatic landforms (within the region of 100 to 270°W, 80 to 87°S). Data coverage of the trough feature includes 114m/pixel MOLA-derived DEM's and shaded relief maps, 105 mappable MOC NA images and several VIS and IR THEMIS images. We have developed several geologic cross-sections across and along the length of the trough to aid in the characterization of bedding attitude and structure of PLD exposed within the trough.

PLD Sequences. Within the trough, we have identified six distinct, overlapping, mappable sequences of PLD. PLD subdivision is based on the topographic expression (e.g., cliff vs. terrace forming, Fig. 1) of layer sequences. The sequences are bounded by marker beds that are laterally continuous throughout the study area and beyond, extending >150 km along the trough, within both enclosing trough walls, as well as within a trough system east of the mapping area. Marker beds can also be seen extending from PLD exposed within the trough floor into scarps of the adjacent spiral troughs. Individual sequences are 28 to >150 m thick; total thickness of the six sequences is several hundred meters. PLD bedding attitudes and features appear structurally controlled (Fig. 2 and 3), exhibiting syn- and antiformal beds with wavelengths of kilometers to tens of kilometers and maximum bedding dip angles of 1.5°. In Figure 3, large wavelength anti-formal bedding and smaller syn- and antiforms within it control the topographic expression of the PLD sequences.

Morphologic Features. Along the trough floor and on the western trough wall are a series of closely spaced ridges and intervening grooves that are described as "wire brush terrain" by [1]. In some cases, the ridges and grooves occur within single layers, but where there is more relief, they cut across many layers (Figure 1 and 2). Some of the grooves form enclosed, lenticular troughs, whereas other grooves appear to be composed of coalescing pits. Intervening ridges in some cases appear to be capped by narrow ridges of probably relatively resistant material. In one instance, where cliff-forming PLD sequences exposed in the eastern trough wall extend onto areas of the trough floor overprinted with ridges and grooves, the more resistant material forms streamlined outliers orientated parallel to the ridge and groove trend. MOC NA images show large boulder-like mounds in places. Transecting pole-ward regions of the trough are a series of east-trending ridges spaced tens of kilometers apart. They are tens of kilometers long, up to several kilometers wide, and have only several meters of local relief. Some of the ridges exhibit moderate sinuosity. A few ridges can be traced almost continuously across the trough flanks and floor, whereas others appear only within the trough or on trough-enclosing, high-standing SPLD. The ridges are overprinted with the ridge-and-groove features. Where imaged by the MOC NA camera, the ridges commonly exhibit layering only on the ridge's south-facing side. At several locations (most notably on the flanks of the trough), ridges are composed of undisturbed PLD that are traceable on both sides of the ridge. In all instances where this is seen, MOLA topography indicates a gentle northward apparent dip of the PLD that make up the ridges—in parallel with subjacent PLD sequences. PLD surfaces, including the "wire brush" terrain and bedding terraces, appear in MOC NA images to be marked by small irregular, shallow pits and alcoves. These features give the PLD a rugged appearance at meters to tens of meters length scales.

PLD Sculpturing. Proposed trough and ridge-and-groove formation mechanisms include glacial scouring and/or streaming, sub-ice volcanism, and eolian activity whereas the west-trending ridges may indicate deformation episodes or in-filled fractures composed of relatively more resistant material [1 and ref within]. Problems with the glacial hypothesis for the ridge-and-groove features include: (1) The supposed basal surface which the moving ice would have scoured is actually within PLD that is well above the base of Planum Australe, yet the underlying PLD does not appear deformed; (2) the trough would have been planed smooth by glaciers; instead, the PLD beds appear terraced; and (3) based on terrestrial examples, the supposed ice stream (marked by the location and extent of ridge-and-groove terrain) should have occurred at or near the margins of the ice sheet [2], not the higher, interior areas of the SPLD. Large collapse pits and crevasses within PLD that should be overlying any hypothetical calderas had sub-ice volcanism occurred are not seen.

The PLD appear to be composed of beds alternating in competency, given: (1) the stair-step slope profile of the PLD, and (2) the alignment of the tops and bottoms of well-developed ridge-and-groove features with the tops and bottoms of individual layers (Fig. 2). The variable competency of the PLD beds may be related to degree of induration, ice composition and structure, and/or concentration of dust particles within an icy matrix. Thus we conclude that eolian scouring chiefly formed the PLD topography. The occurrence of ridge-and-groove terrain within the trough may be attributable to enhanced intensity and longevity of down-slope winds that have carved dip slopes of friable material. However, the ridge-and-groove terrain does not seem to be actively developing; instead, fine-scale pitting and scarp retreat appears to be the most recent observed landform development, perhaps due to back wasting and sublimation of surface or near-surface ice. An eolian scouring trough-formation mechanism would indicate that several hundred meters of SPLD material has been removed (Fig. 2). In Figure 3, the east-trending ridge occurs at the presumed crest of an anticline. This association, and that PLD is typically only seen on the south side of the ridges indicates that the ridges are the erosional expression of north-dipping SPLD beds.

Relative Timing. Along the length of the radial trough are transecting and evenly spaced topographic swales that connect with and are of the same dimensions and orientations, as that of adjacent spiral trough features within Planum Australe. Within the radial trough, swale crest elevations are 100's of meters lower than their counter parts within the spiral troughs. We postulate that the radial trough post-dates initialization of spiral trough formation and that the swales are the remnants of spiral trough features that had previously extended into regions now occupied by the radial trough. If the spiral troughs have formed by ice-flow processes [3], the undisturbed, continuous bedding contacts that extend from the radial trough into the spiral troughs indicate that since commencement of trough formation, ice flow has not occurred. Erosion of the spiral troughs may be facilitated by along-trough winds (as supported by the streamlined morphology of capping SPLD located on the crest of a spiral trough at 250°W, 83°S) or sublimation of equator-facing slopes. However, we see no evidence for the redeposition of layers on pole-facing slopes [4].

Summary. Our investigation of the trough in Planum Australe that contains distinctive ridge-and-groove ("wire brush") terrain suggests that the PLD:

(1) Consist of layers of variable competency
(2) Include distinctive marker bends traceable for >100 km
(3) Have not been eroded significantly by glacial scour
(4) Do not show deposition of spiral trough wall material on pole-facing slopes
(5) Have experienced significant eolian erosion, including the development of the broad radial trough, the ridge-and-groove terrain, and east-trending ridges by down-slope winds on dip slopes in beds of alternating competency
(6) Radial trough emplacement occurred after spiral trough formation began; their development may include eolian erosion and/or sublimation
(7) Have undergone slope backwasting to reveal beds of variable erosional resistance
(8) Most recently have been dominated by pitting and scarp retreat that may be related to localized removal of ice-rich material

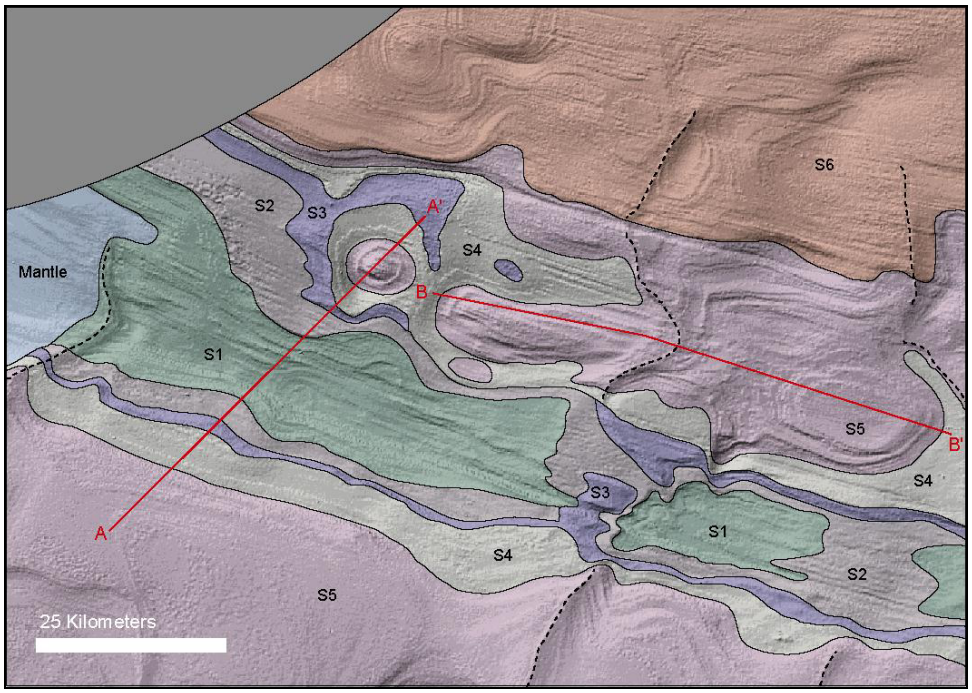

Figure 1. Geologic map of part of the north-trending radial trough east of Chasma Australe. The east-trending ridges are highlighted with a dashed line.

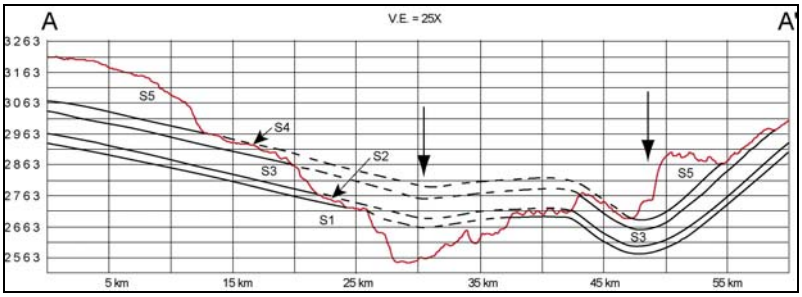

Figure 2. Elevation in meters. Maximum bed dip angle is ~1.5°. The large arrows highlight the axis location of two north-trending synclines.

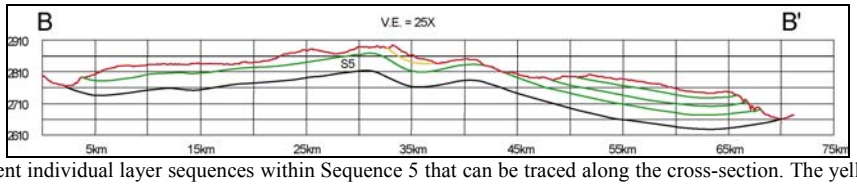

Figure 3. Green lines represent individual layer sequences within Sequence 5 that can be traced along the cross-section. The yellow line is drawn to highlight bedding orientations where the SPLD crosses an east-trending ridge. The PLD descend over 200 m towards the margin of Planum Australe and the average bed dip angle is ~0.5°.

References: [1] Koutnik M.R. et al., (2003) 6th Intl. Mars Conf. #3134 [2] Hourmark-Nielson, M. et al., (2001) Paleo-Ice Stream International Symposium. Pg. 35 [3] Fisher, D. A. (1993) *Icarus* **34**, 501-511. [4] Howard, A.D. (2000). *Icarus* **144**, 267-288.

CHASMA AUSTRALE, MARS: FORMATION BY SUCCESSIVE HEADWARD THERMO–EROSIONAL COLLAPSES.

S. van Gasselt, R. Jaumann, *German Aerospace Center, Institute of Planetary Research (Stephan.vanGasselt@dlr.de)*.

Abstract: The development of the south polar Chasma Australe re-entrant has been discussed for several years and a variety of theories including eolian, aquatic, subglacial and tectonic mechanisms have been proposed for its formation. Morphological observations and studies of recent imagery support the idea of successive headward erosion and removal of volatile–rich sub–surface material combined with collapse and eolian blow–out processes.

Introduction: The south polar Chasma Australe is a prominent arcuate elongated trough. Discussed models are formation by eolian processes [2, 3], aqeuous carving [4, 5], subglacial volcanic processes [5, 6] as well as tectonically triggered catastrophic outflow events [1] and basal melting [13]. In this work we provide some aspects to contribute to the understanding of its development. We have mapped the circum–Chasma Australe region on the basis of available imagery (Viking, Global Surveyor MOC, Odyssey THEMIS) at all resolutions and performed morphometric measurements on the basis of Laser Altimetry topographic data (MOLA) to evaluate outflow models proposed for the Chasma Australe development. A detailed description of the general morphology of the Chasma Australe has been provided by [1].

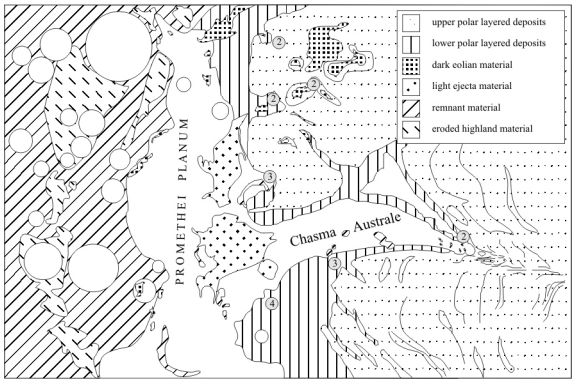

Fig. 1: Map of geomorphologic units of the Chasma Australe region, Promethei Planum and adjacent units. The Chasma Australe system is accompanied by several unlabeled Chasmata (2-4) to the east and west. Several elliptical and circular shaped depressions are located near the heads of secondary (2) re–entrants which indicate identical formation processes. Earlier stages of development (3-4) are presented by small third generation re–entrants. Light material near the terminus of Chasma Australe is connected to impact ejecta, which might be rich in volatiles, as lobate ejecta blankets indicate as well. Lineations south of the head of Chasma Australe.

Geomorphologic and geologic setting: The Chasma Australe is an arcuate and elongated steep sided depression with a length of ≈500 km and a width of 16.5 km at its head and 93 km at its terminus. The Chasma head begins near $-82°$S/90°E and reaches down to 71°S/86°E with an opening angle of $\approx 30°$. It terminates in the Promethei Planum, a large circum-polar basin. The head of Chasma Australe is a well–defined, almost circular depression at an elevation of 2500 m with a depth of 950 m. Inside the U–shaped depression a secondary almost circular depression with a depth of ≈100 m and a diameter of ≈5 km appears. The Chasma terminus is situated at an elevation of ≈1060 m and is marked by a lobate–shaped remnant of possible base rock material.

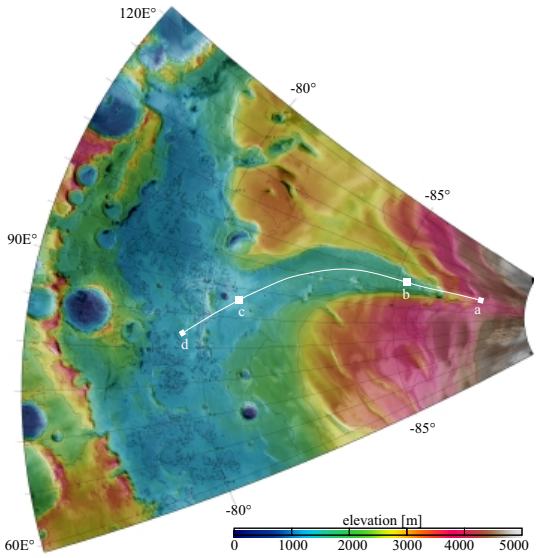

Fig. 2: Topographic map of Chasma Australe, Promethei Planum and adjacent units. Line a-b-c-d marks the profile discussed in the text.

The trough cuts into the Amazonian aged polar layers (Apl), which have been exposed mainly on the eastern flank. The basis of the re–entrant consists of the Hesperian aged Upper and Lower Dorsa Argentae Formations (Hdu and Hdl) [7].

Observations: From its head to its terminus the Chasma covers an area of $\approx 93.6 \cdot 10^3$ km^2. MOLA measurements have shown that $\approx 28.4 \cdot 10^3$ km^3 of material have been removed from the trough. The main trough (profile b:c) has a length of $\approx$ 300 km and slopes with an average angle of $0.06°$ ($S = 0.00112$) (see fig. 3). For comparions reasons we estimated discharge values Q[1] with the help of eight Chasma cross–sections and obtain values ranging from $3.67 \cdot 10^8 m^3 s^{-1}$ to $4.73 \cdot 10^9 m^3 s^{-1}$, depending on the Manning coefficient n (0.03-0.05 [11]) and the definition of the hydraulic radius R. For velocities v we obtained values ranging from $37 ms^{-1}$ to $68 ms^{-1}$. The values show a larger range of estimated peak discharges but they are of the same order as calculations by [1] and estimations for outflow systems in mid latitudes [9]. We obtained higher velocities and slightly larger discharge values. The Chasma floor has a rough small–scale surface texture.

[1](using $v = \left[(g_m RS) / \left(g_e n^2 R^{-1/3}\right)\right]^{1/2}$according to [11], with velocity $v[ms^{-1}]$, Mars/Earth gravity $g_{m/e}[ms^{-2}]$, hydraulic radius $R[m]$, bed slope $S[-]$, Manning coefficient $n[-]$).

Except for several crater chains in East–West direction only elongated ridges almost perpendicular to the proposed outflow can be observed. We find no streamlined islands as classic features for mid–latitude outflow channels and we have no evidence for outflow–parallel ridges and terraces as a high energetic flow would have caused.

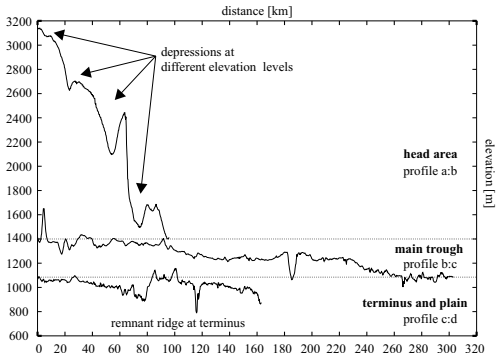

Fig. 3: Length profile of the Chasma Australe head, the main trough and the southern parts of the Promethei Planum.

In an abundance of MOC–NA imagery we observe a pattern of linear, radial and polygonal crack patterns [10] accompanied by cicular and elongated depressions in the vicinity of the Chasma walls and other re–entrants of the south polar region. The crack pattern is aligned parallel to the polar layer outcrops and becomes more densely spaced towards the Chasma walls. These fractures occur mainly near to the southern and eastern (steeper) walls. Linear fracture are connected to elongated depressions and radial fractures are connected with circular depressions. In lower resolution imagery (MDIM resolution) we observe a set of lineaments and large circular depressions south of the Chasma Australe head. The lineaments are exposed polar layer deposits and circum polar troughs which seem to bend in the headward direction of the Chasmata. Fig. 3, profile a:b shows several depressions south of the Chasma head. Each base is situated on a higher elevation level which indicates a headward progressing process of material removal. Near the western walls of Chasma Australe several remnants break through a mantling deposit (s. fig. 2). Between remnant rock and Chasma wall the polar layered deposits remain completely intact.

Conclusions: For the Chasma Australe we propose a successive headward thermo–erosional formation which has been initiated at the Promethei Planum boundary. Sapping processes due to subsurface removal of volatiles could be responsible for collapses and depressions which are aligned in the main directions of several observed Chasmata. Material has been removed afterwards in the direction of the Promethei Planum during several stages similar to the model of supra–glacial erosion by [8]. (1) Although discharge quantities are similar to mid–latitude outflow channels, the general morphology (smoothness, curvature, profile) differs immensly from the well defined known outflow channels. (2) Polar layers remain intact near crucial locations, we have no signs for streamlined islands, groove casts, secondary inner–valley channels or deposits at the terminus towards the Promethei Planum. We find some hints for (3) volcanic influence (crater chains on the Chasma basis and volcanic remnants [12]). Cracks, fissures and small basins near the walls indicate subsurface instabilities in the proximity of the Chasma. The fracture pattern favours the idea of contraction cracking of the surface material, either due to dessication or due to freezing processes of the surface as analogue to terrestrial ice wedge polygonal nets. The depressions indicate either removal of surface material due to deflation, similar to terrestrial pans, sublimation processes or subsurface removal of volatiles and subsequent collapse.

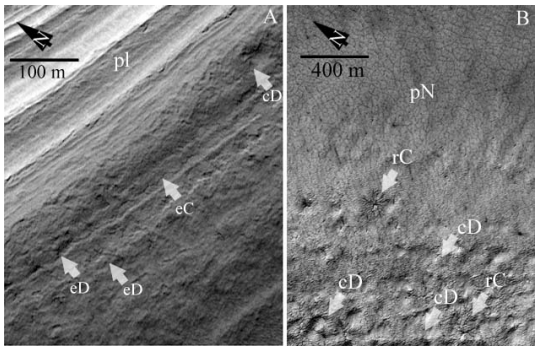

Fig. 4: Selected MOC–NA images at the head of Chasma Australe. (A) E12/02439: The eastern wall shows the layered units (Apl) and presents a pattern of elongated (eD) and circular depressions (cD), as well as elongated cracks (eC) parallel to the layering. (B) E11/01508: Image south of the Chasma's circular head. The polygonal network (pN) is gradually changing to aligned circular depressions and some occurences of radial cracks (rC).

Volcanic processes could be main trigger mechanisms for volatile removal in the subsurface, contraction–cracking and collapse might be bound to this process. Furthermore, eolian transport has a major influence on erosion and mantling the topography. Small–scale cracking and collapse structures are not mantled by eolian material although the overall surface appears very deflated, so even processes of contraction cracking and collapse could occur at present time. Open questions are adressed to the nature of cracking origin (dessication or (CO_2)ice wedges) and the removed material below collapse structures.

References: **[1]** Anguita, F. et al. (2000) *Icarus* **144**, 302-312. **[2]** Cutts, J. A. (1973) *J. Geophys. Res.* **78**, 4211-4221. **[3]** Howard, A. D. (1980) *Icarus* **50**, 161-215. **[4]** Wallace, D. and C. Sagan (1979) *Icarus* **39**, 385-400. **[5]** Clifford, S. M. (1987), *J. Geophys. Res.* **92**, 9135-9152. **[6]** Benito, G. et al. (1997) *Icarus* **129**, 528-538. **[7]** Tanaka K. L. and D. H. Scott (1987) *US Geolog. Surv.*, Map 1-1802-C, Washington D. C. **[8]** Costard, F. et al. (2003) *Lun. Planet. Sci. Conf. XXXIV, #1354*, Houston. **[9]** Komatsu and Baker (1997) *J. Geophys. Res.* **102**, 4151-4160. **[10]** van Gasselt, S. et al. (2003) *3rd Mars Polar Sci. Conf., this volume*. **[11]** Komar, P. D. (1979) *Icarus* **37**, 156-181. **[12]** Ghatan, G. J. and J. W. Head (2002) *J. Geophys. Res.***107**, 10.1029/2001JE001519. **[13]** Fishbaugh, K. et al. (2000) *Lun. Planet. Sci. Conf. XXXI, #1206*, Houston.

AMAZONIAN GEOLOGIC HISTORY OF THE NORTH POLAR CAP OF MARS: STRATIGRAPHY, MELTING, AND RETREAT Kathryn E. Fishbaugh[1] and James W. Head III[1], [1]Brown University, Dept. Geol. Sci., Box 1846, Providence, RI 02912, kathryn_fishbaugh@brown.edu, james_head_III@brown.edu

Introduction: Mariner 9 [1,2] and Viking era studies [e.g., 3] showed the polar caps to consist of layers with varying amounts of dust and ice, termed the polar layered deposits (Apl), and a residual polar cap (Api) consisting of ice and dust overlying these [4]. In the north, this residual cap consists of water ice and in the south of water and CO_2 ice [4], yet CO_2 clathrate may also compose a percentage of the Apl and residual ice at both poles [5]. Most authors believe that the variability in dust content within the Apl is to some degree controlled by orbital oscillations [6-8]. Only recently have researchers considered the martian polar caps as possibly behaving similarly to terrestrial ice caps, both glaciologically and geologically. *Tanaka and Kolb* [9] and *Kolb and Tanaka* [10] have outlined a possible geologic history of the poles, suggesting that melting and flow have not occurred. Yet, several authors have estimated ice flow rates, of mm to meters/yr [11-13], and Fisher [14] has put forth the idea that ice flow may play a crucial role in the forming of the northern spiraling troughs. Just as terrestrial ice sheets experience meltwater outbursts in the form of jökulhlaups, Chasma Boreale may also have been formed in part by melting of the Apl (possibly due to volcanic eruption) and outflow [15-17]. There is also geologic evidence for at least one stage of retreat of the north polar cap [18,19]. Thus, the martian north polar cap has a much more complex and Earth-like history than simple accumulation of residual ice and dust.

A major outstanding question in the study of the north polar cap is, "When did all of this occur?". *Tanaka and Scott* [4] have placed the beginning of Apl deposition for both caps in the Late Amazonian, and *Herkenhoff and Plaut* [20], based on crater counts, have estimated maximum surface ages of 7-15 x 10^6 yrs. (south) and <100 x 10^3 yrs. (north). The goal of our research thus far has been to piece together a possible history of the north polar cap from the end of Vastitas Borealis Formation (VBF) deposition in the Late Hesperian to the current estimates of the beginning of Apl deposition nearly 3 billion years later in the Late Amazonian. Thus, we have studied the major stratigraphy of the polar deposits, the evidence for growth and retreat of the polar cap, and its melting history.

Stratigraphy: As described above, the polar cap consists of two major units: the polar layered deposits (Apl) and the residual ice (Api) overlying these. *Howard et al.* [21] have described the stratigraphy of the Apl in detail using Viking data. The darker, dustier layers are laterally continuous and contain an unknown percentage of dust. Layer thicknesses vary; Viking images revealed major layers on the order of 5-25 m thick, while MOC has shown layer thicknesses down to the limit of resolution (~2 m) [22,23]. Recently, a darker, layered unit has been found to lie beneath the Apl [22,10,24,25]; *Tanaka et al.* [26] term this unit "polar layered deposits 1" (Apl_1) and give it an Early Amazonian age. We have referred to this unit as the basal unit. Building upon these previous studies of the basal unit, we have continued to investigate its major characteristics [27].

The basal unit consists of alternating light and dark layers. The darker layers are much thicker (10s of meters) and less easily eroded than the thinner ones which may consist of the ubiquitous planetary dust. Steep slopes (some near 40°) indicate possible cementation by water ice. Individual layers also erode at different rates, and some of the lower layers show evidence of eolian erosion. Since the basal unit is exposed in troughs within Olympia Planitia, the sublimation and wind erosion which produced the trough [28] is able to erode the basal unit as well. This erosion has left behind pits, ridges, residual mesas, and yardang-like forms.

The close geographical association of basal unit outcrops with the northern dunes suggests that the basal unit is probably the source for these dunes [24], just as *Thomas and Weitz* [29] found that the lower Apl was probably the dune source (before the basal unit was discovered). The Apl also appear to unconformably overlie the basal unit since the basal unit layers pinch-out along the contact, indicating that major erosion may have taken place between the end of basal unit deposition and the beginning of Apl deposition. It is also possible that deposition of the basal unit occurred in irregular patches, rather than in continuous layers, creating the illusion of an unconformity. Dark lenses found within the lower Apl layers may be dunes which eroded from the basal unit and migrated onto the young, still-forming Apl.

The best exposures of the basal unit lie within the troughs bordering and extending into Olympia Planitia and within the arcuate scarps at the head of Chasma Boreale. At its thickest point, the basal unit is approximately 400 m thick (1100 m, including Olympia Planitia) and pinches out somewhere near Chasma Boreale. According to *Byrne and Murray* [24], Olympia Planitia consists wholly of the basal unit.

We have investigated several theories of formation of the basal unit [30], including 1) eolian deposit, 2) outflow channel/oceanic deposit, 3) incorporation into basal ice, and 4) a remnant of several stages of polar cap retreat, and find that the latter scenario is most likely. Formation of the basal unit accounts for some of the Amazonian history of the north polar cap.

Melting of the Polar Cap: Using Viking data, two different theories on the formation of Chasma Boreale have arisen: katabatic wind erosion and sublimation [28] and melting and outflow [15,16]. We have examined these and formation by glacial flow and ablation using primarily MOLA data and find that the most likely mechanism of formation is a combination of sublimation, katabatic wind erosion, melting, and outflow [17]. The cause of such melting is still unknown but candidate triggers include: 1) volcanic eruption, 2) climate change of a scale large enough to cause melting, 3) incorporation of salts into the

lower layers, and 4) pressure melting due to the presence of a thicker cap. The basal unit may have played a crucial role in the creation of Chasma Boreale as it may have affected placement of water reservoirs and transportation of that water. In addition, much of the basal unit has been eroded by formation of Chasma Boreale; the floor and lobate deposits at the mouth may consist of modified lower layers of the basal unit. If the north polar cap underwent at least one stage of relatively large-scale melting, then this may have contributed in part to polar cap retreat.

Retreat of the North Polar Cap: We have described geologic evidence for at least one stage of polar cap retreat [19,31]. Unusual, rough, knobby depressions south of Olympia Planitia resemble kame-and-kettle topography, formed on Earth by the deposition of englacial sediment and melting of blocks of ice left by glacier retreat. Remnants of polar material (mapped by *Tanaka and Scott* [4]) also lie within and near the kame-and-kettle–like topography. Previously, we described Olympia Planitia as consisting of remnant Apl covered by sublimation lag now reworked into dunes. Based on subsequent studies of the basal unit, we consider it more likely that Olympia Planitia consists of basal unit material which may itself be a remnant of several stages of polar cap retreat.

Retreat of the polar cap plays a crucial role in its history, because it implies that the north polar cap may not have just appeared in the Late Amazonian but instead may have been influencing the hydrologic and climatic cycles of the planet for much longer and may have waxed and waned with changes in climate.

Possible Scenarios of North Polar Cap History: We have outlined four possible scenarios for north polar cap history [32]. (1) Deposition of the polar cap is a recent event, requiring that climate has only just become favorable for polar cap deposition. We find this case unlikely since a climate largely controlled by orbital parameter variations would not have undergone an overall, large-scale change during the Amazonian other than the smaller scale variations caused by the orbital parameter variations [8]. In addition, in this case, triggers needed to cause melting and retreat would be difficult to achieve in such a short time period. (2) Polar wander [33] has recently brought the caps to their present positions. (3) The polar cap is oscillating, waxing and waning with large changes in orbital parameters, the current polar cap being only the latest manifestation of caps that have come and gone since perhaps the Early Amazonian. Ice deposits may even form at lower latitudes during periods of high obliquity [34]. One possibility is that the major layers of the basal unit each represent a lag left by the retreat of one stage of the polar cap. Since the basal unit is exposed in Chasma Boreale and has been eroded by chasma formation, any melting involved in carving the chasma would have occurred after the last major stage of retreat but may also have occurred during previous stages. *Jakosky et al.* [35] modeled sublimation of the polar cap and found that a pure ice cap of the current Apl thickness could sublimate entirely within 50 x 10^3 yrs. at high obliquities (>45°). (4) The lower layers of the polar cap were deposited in the early Amazonian, and deposition has continued since then; crater counting may reveal only their surface age. In this case, the cap may have undergone more than one stage of partial retreat, and processes such as flow and relaxation [36] may be erasing craters and making the surface appear even younger than it is.

Comparison with the South Polar Cap: The south polar cap shares some characteristics with its northern counterpart. Evidence in the form of esker-like ridges, remnant volatile-rich material, and drainage channels indicate possible retreat of southern polar deposits during the Hesperian [37]. Chasma Australe bears a striking large-scale morphological similarity to Chasma Boreale and thus may also have been formed by melting, yet detailed similarities are few, possibly due to the lack of a southern basal unit and thus lack of a significant source for outflow deposits. *Kolb and Tanaka* [10] cite a dearth of features formed by flow and undisturbed layer sequences in the walls of the chasma as evidence against formation by melting and outflow. Our preliminary searches have shown no evidence for a southern basal unit. Possibly, subsequent stages of growth and retreat of the south polar cap during the Amazonian left no basal unit, though there is evidence for small scale growth and retreat during this time [38]. Perhaps early retreat of the southern deposits left such a thick lag that later retreat was significantly retarded. However, there may exist a much smaller southern basal unit that has not yet been exposed. Further studies should include more comparisons with the south polar deposits so that the ideas developed about the north polar cap can be tested.

References: [1] Soderblom, L. et al. (1973), *JGR* 78, 4197-4210. [2] Cutts, J. (1973) *JGR* 78, 4231-4249. [3] Thomas, P. et al. (1992), in *Mars* (ed. By H. Kieffer et al.), 767-795, U of Ariz. Press, Tucson. [4] Tanaka, K. and D. Scott (1987), *U.S.G.S. Misc. Inv. Ser. Map I-1802-C*. [5] Hoffman, N. (2000), *Icarus* 146, 326-342. [6] Blasius, K. et al. (1982), *Icarus* 50, 140-160. [7] Cutts, J. et al. (1982), *Icarus* 50, 216-244. [8] Laskar, J., et al. (2002), *Nature* 419, 375-377. [9] Tanaka, K. and E. Kolb (2001), *Icarus* 154, 3-21. [10] Kolb, E. and K. Tanaka (2001), *Icarus* 154, 22-39. [11] Pathare, A. and D. Paige, *2nd Int. Conf. Mars Polar Sci. and Exp.*, LPI Contrib. 1057, pg. 79. [12] Hvidberg, C. (2003), *Annal. Glaciol.*, in press. [13] Greve, R. et al. (2003), *Planet. and Space Sci.*, in press. [14] Fisher, D. (2000), *Icarus* 144, 289-294. [15] Clifford, S. (1987), *JGR* 92, 9135-9152. [16] Benito, G. et al. (1997), *Icarus* 129, 528-538. [17] Fishbaugh, K. and J. Head (2002), *JGR* 107, 10.1029/2000JE001351. [18] Zuber, M. et al. (1998), *Science* 282, 2053-2060. [19] Fishbaugh, K. and J. Head (2000), *JGR* 105, 22455-22486. [20] Herkenhoff, K. and J. Plaut (2000), *Icarus* 144, 243-255. [21] Howard, A. et al. (1982), *Icarus* 50, 161-215. [22] Malin, M. and K. Edgett (2001), *JGR* 106, 23429-23570. [23] Milkovich, S. and J. Head (2003), *LPSC* 34, #1342. [24] Byrne, S. and B. Murray (2002), *JGR* 107, 10.1029/2001JE001615. [25] Edgett, K. et al. (2003), *Geomorph.* 52, 289-297. [26] Tanaka, K. et al. (2003), *JGR* 108, 10.1029/2002JE001908. [27] Fishbaugh, K. and J. Head (2003), *6th Mars Conf.*, #3137. [28] Howard, A. (2000), *Icarus* 144, 267-288. [29] Thomas, P. and C. Weitz (1989), *Icarus* 81, 185-215. [30] Fishbaugh, K. and J. Head, *6th Mars Conf.* #3141. [31] Fishbaugh, K. and J. Head (2001), *LPSC* 32, #1426. [32] Fishbaugh, K. and J. Head (2001), *Icarus* 154, 145-161. [33] Schultz, P. and A. Lutz (1988), *Icarus* 73, 91-141. [34] Jakoksy, B. and M. Carr (1985), *Nature* 315, 559-561. [35] Jakosky, B. et al. (1995), *JGR* 100, 1579-1584. [36] Pathare, A. and D. Paige (2003), *LPSC* 34, #2051. [37] Head, J. and S. Pratt, *JGR* 106, 12275-12299. [38] Head, J. (2001), *JGR* 106, 10075-10085.

USING MARS ORBITER LASER ALTIMETER DATA TO DETECT SUBGLACIAL FEATURES AT THE RESIDUAL NORTH POLAR ICE CAP. M. C. Payne[1] and J. D. Farmer[1], [1]Department of Geological Sciences, Arizona State University (PO Box 1404, Tempe, AZ, 85287, USA, mcpayne@asu.edu, jfarmer@asu.edu).

Introduction: Digital Elevation Models (DEMs) constructed from Mars Orbiter Laser Altimeter (MOLA) data are a valuable tool in the analysis of surface geomorphic features. When formatted for use in a Geographical Information Systems (GIS) software package, such as ESRI's ArcView, MOLA data can be used to compose DEMs. In turn, the DEMs can be used to create contour maps, to create profiles through features of interest, and to generate hill-shaded views that provide an image-like perspective of selected areas. Furthermore, DEMs eliminate many problems associated with photographic images, such as over- or underexposure, sun angle, and high albedo.

In this study, we examined an area near the margins of the north polar cap in Olympia Planitia, using MOLA DEMs. We show that in marginal glacial areas where the ice is thin, MOLA detects variations in subglacial land surface topography, including a variety of distinctive geomorphic features (e.g. impact craters, fluvial channels, coniform features of probable volcanic origin, etc.). We offer a simple model to explain why MOLA is sensitive to subglacial geomorphology, and then demonstrate the potential for determining important aspects of the geologic history of polar regions obscured by surface ice and snow, using superpositional relationships apparent in MOLA DEMs.

Study Area: The region of study is located along the margin of the Martian north polar cap. This broad area, named Mare Boreum, consists of a perennial polar cap of H_2O ice, underlying CO_2 ice [1], surrounded by four distinct polar sand seas [2, 3] and a remnant polar cap margin extending from ~ 80°-75° N latitude and ~ 105°-255° W longitude.

The site discussed here is centered at ~77° N, 183° E. A feature resembling a small volcano, and a bifurcated valley, are visible in Viking images of this area. MOLA data for the site were used to test hypotheses for the origin of these features. In the process of that work on surface features, a number of subglacial geomorphic features were also detected in DEMs.

Methods: MOLA data points were input into ESRI's ArcView GIS software to create digital elevation models (DEMs) that offer an image-like view of the study site (Figure 1). The craters visible in the DEMs are actually subglacial features not visible in Viking or MOC images (Figures 1). Clearly, these subglacial features were detected by MOLA, establishing that DEMs can be used to see the geomorphology of the sub-ice features in this marginal region of thin ice (average ice thickness at the site ~100-300 m). Furthermore, the DEMs allow geomorphic measurements (such as topographic profiling) of the observed features, further facilitating their characterization.

Figure 2 explains why MOLA data is sensitive to sub-ice features in polar cap margin environments. As ice and snow accumulate over a topographical surface, the surface topography of the ice mirrors the underlying topography. As ice/snow cover increases in thickness, the underlying topography is progressively damped out, becoming more subdued. When the accumulated ice/snow cover has reached a significant thickness relative to the total relief of the underlying topography, sub-ice topography is no longer expressed at the surface. Altimetry data and DEMs of the surface of the north polar cap revealed that MOLA is indeed very sensitive to subglacial topographic features, such as the craters and channels shown in Figure 1. The form of the features is easily discernable in DEMs, as are superpositional relationships of the features. We conclude that the technique of using MOLA data to study subglacial features in marginal polar regions where ice thicknesses are less than the relief of the buried surfaces, provides a new way of mapping geomorphic units in such regions, and for reconstructing geologic history.

Age relationships/Geologic history: The subglacial craters and channels documented in the present study lie within the "mantled smooth plains material" mapped by Dial [4], which was assigned the age of mid-Amazonian. More recently, Herkenhoff and Plaut [5] used crater-counting techniques to derive an age for the north polar-layered deposits and residual cap of between 74 ka and 147 ka. Therefore, it may be concluded that the features discussed here are certainly younger than mid-Amazonian, and may be much younger.

Cross-cutting relationships of geomorphic features observed in the hill-shaded DEMs suggest that the 18 and 44 km diameter craters are the oldest features observed in the study area. Although glacial advances and retreats of the north polar ice cap are likely to have substantially modified the overall morphology of these craters, their characteristic form is obvious. Cross-cutting relationships suggest that the channels that breach these craters are younger.

Subglacial fluvial activity (e.g. basal melting environments of Clifford [7]) typically creates positive-relief, ridge-like features (e.g. eskers). However, most

of the channels observed in the region of study are interpreted to be pre-glacial and could have been formed by either: 1) fluvial systems associated with impact-generated hydrothermal systems (e.g. [6]) or 2) surface flows unrelated to impact hydrothermal processes. It may be noted that the northern channel has a more pristine appearance than the sinuous channel to the south and therefore may be younger.

A sinuous ridge found at the study site is the strongest candidate for an earlier period of subglacial fluvial activity and could be as young as the last glacial advance in this area. A pristine impact crater appears to be superimposed on this feature and is likely a post-glacial occurrence. This impact crater (and several nearby impact craters) overlie all other features in the region, and thus, are the youngest features observed.

Coniform features in the study are interpreted to be small volcanoes. This interpretation is supported by the presence of summit craters in profiles of these features. The concentration of these features in one area may indicate the presence of a single volcanic field. The timing of observed coniform features is difficult to assess. They predate the pristine impact craters, but post-date the heavily degraded 18 and 44 km diameter craters. However, their age relationship to the channels is ambiguous. It is possible that their formation overlapped with the channels, although they could also be younger.

Summary: The analysis of MOLA DEMs of ice-covered regions marginal to the north polar cap has proven useful for interpreting the geologic history of the region beyond that based on imaging alone. Superpositional relationships suggest that an ancient cratered terrain, formed during a pre-glacial era, underlies the area of the remnant north polar ice cap.

To summarize the characteristics of the region of study, the presence of subglacial channel-forms revealed by MOLA data almost certainly indicates that the surface underlying the remnant cap was modified by flowing surface water in the distant past. The presence of a sinuous ridge interpreted to be an esker suggests that subglacial fluvial activity continued in the region through the most recent glacial advance. Coniform features in the area are interpreted to be of volcanic origin, suggesting that subsurface magmatic sources could have sustained subsurface hydrothermal systems and surface outflows for some time.

The valley forms observed in DEMs suggest that they formed by surface flows of water during a pre-glacial epoch subsequent to the formation of the oldest craters. The coniform features, interpreted to be volcanic constructs, likely formed around the same time.

An analysis of the geomorphic features in this area (utilizing MOLA data) suggests that liquid water has existed in this region for a long time. This observation is particularly relevant for NASA's exploration strategy to "follow the water" as a basis for understanding the potential for past of present habitable environments for Martian life.

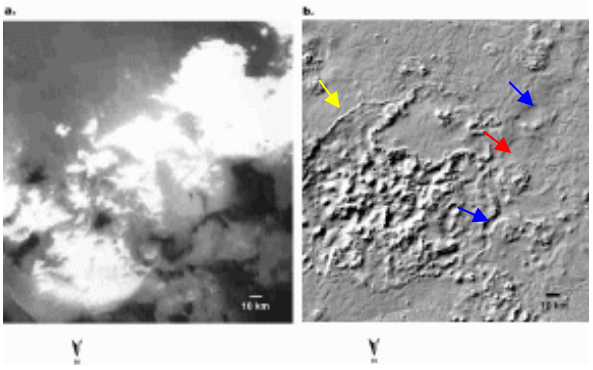

Figure 1. The study site is shown above using a) MOC wide angle visible image data, and b) a hill-shaded view of a DEM constructed from MOLA point data. The scales and areas of figures a and b are identical. It is obvious that the MOLA data provides a wealth of geomorphic information (such as the revelation of craters (red arrow), channels (blue arrows), and other landforms such as a possible esker feature (yellow arrow)) which is obscure or invisible in camera images.

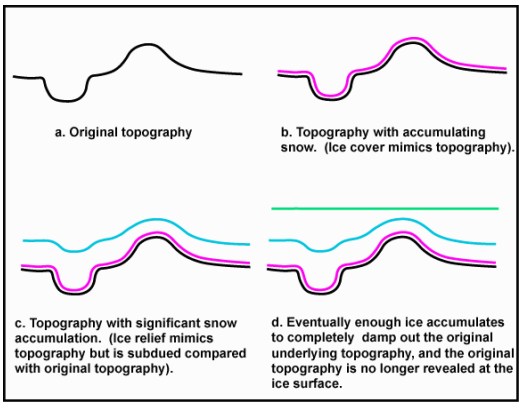

Figure 2. Graphical representation of how ice mimics topography allowing detection of subglacial features by MOLA.

References: [1] Thomas P. et al. (1992) *Polar deposits of Mars*, in *Mars*, H.H. Kieffer et al., Editors, 767-795. [2] Tsoar H. R. et al. (1979) *JGR, 84,* 8176-8180. [3] Lancaster N. and Greeley R. (1990) *JGR, 95,* 10,921-10,927. [4] Dial A. L. (1984) *Geologic map of the Mare Boreum area of Mars; scale 1:5,000,000*, United States Geological Survey. [5] Herkenhoff K. E. and Plaut J. J. (2000) *Icarus, 144,* 243-253. [6] Brakenridge G. R. et al. (1985) *Geology, 13,* 859-862. [7] Clifford S. M. (1987) *JGR, 92,* 9135-9152.

ALBEDO FEEDBACK IN THE PATTERNING MECHANISMS OF MARTIAN POLAR CAPS. Felix S. L. Ng, Maria T. Zuber, *Department of Earth, Atmospheric and Planetary Sciences, Massachusetts Institute of Technology, Cambridge MA 02139, USA (felix@mit.edu)*.

Introduction. Both the north and south polar caps on Mars display conspicuous patterns of spiraling troughs on the surface (Fig. 1), and their origin is largely unexplained. Here we examine the hypothesis that such morphology could be the result of a spatial instability. By modeling the interaction of polar ice with the Martian atmosphere, we show that an albedo feedback (associated with dust) can lead to relaxation oscillations in the coupling between surface mass exchange, radiative heat balance and air moisture regulation. Under favourable conditions, this temporal behaviour is manifest on the surface of the residual ice caps as alternating domains of sublimation and condensation, whose evolved forms mimic the observed (dark) troughs and their adjacent (light) smooth terrains; their expected orientation and topography are broadly consistent with the actual pattern. The mechanism finds observational support from stratigraphic relationships in the cap deposits [1] and recently inferred wind patterns, and may offer useful insights for developing more complex models.

Background. Understanding large-scale patterning of the Martian ice caps is an important step towards deciphering their history, because it reflects the unique conditions under which the exchange of volatiles (CO_2 and H_2O) and dust between ground and atmosphere occurred in the polar regions. In addition, ice cap internal layers exposed on the equator-facing trough walls (or 'scarps') may contribute a valuable record of Martian climate cycles [2,3]. The age and rate of pattern formation can also be used to constrain other polar processes.

It is generally thought that the observed system of troughs migrates poleward due to isolation-driven ice sublimation at the scarps, while ice accumulates on inter-trough areas [4]. Previous studies explored the role of these processes in creating the spiral planform [5] and their effect on ice cap internal stratigraphy [6,7], but it remains unclear as to how the troughs were initiated and maintained, and what governs their spacing.

It is likely that the troughs developed via a positive feedback resulting from surface processes rather than from ice flow, for the latter has the tendency to suppress surface undulations. This idea is supported by steady flow modeling of the north polar cap [7]: to sustain scarps, ablation at their base and accumulation at their top must be imposed. Presumably, wave-like propagation of the scarp topography requires a similar mass balance configuration.

Mathematical Model. The feedback studied here connects the regulation of surface albedo a to the direction of mass transfer at the ice surface — that is, whether $\dot{m} > 0$ or $\dot{m} < 0$, if $\dot{m}$ denotes the rate of sublimation. Drawing on an earlier description of radiative energy balance and the sublimation process [8], we calculate $\dot{m}$ from the equations

$$I_n(1-a) = \sigma T^4 + \dot{m}L, \tag{1}$$

$$\dot{m} = D(p_s - \phi)\sqrt{\frac{M_w}{2\pi k T^{1/2}}}, \tag{2}$$

in which I_n is the incident solar flux (corrected for surface slope), T is the surface temperature, ϕ is the partial vapour pressure of CO_2 or H_2O in the atmosphere (whichever ice-type is being considered), and p_s is the saturation vapour pressure, $= c_0 e^{-c_1/T}$. Model constants are explained in ref. [8].

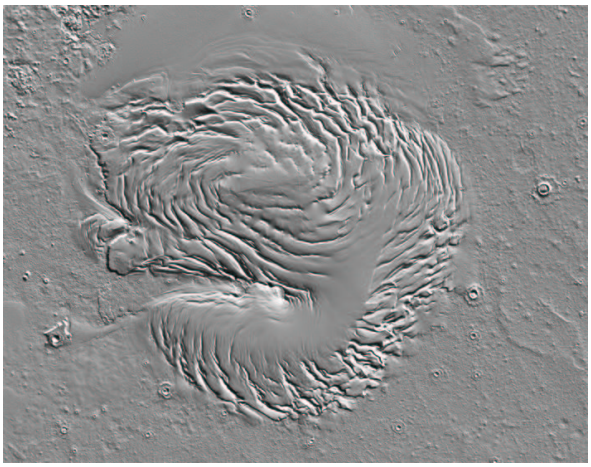

Figure 1: *Shaded relief image of the Martian northern polar region, showing spiral chasms. Courtesy of MOLA Science Team.*

A crucial control on the surface albedo is the dust content of the dirty ice. We envisage sublimation to promote a low albedo ($a = a_1$) by exposing dust at the surface, and condensation to have the opposite effect through burial of the dust (raising a to a_2). While this process can be modeled in detail, here it is sufficient to suppose that such albedo change can be achieved by removing/depositing an ice or snow layer of thickness Δ, and then an appropriate description is

$$\frac{\Delta}{|\dot{m}|}\frac{da}{dt} + a = \frac{a_2 + a_1}{2} - \frac{a_2 - a_1}{2}\mathrm{sgn}(\dot{m}). \tag{3}$$

Analysis of Equations (1)–(3) shows that for a given insolation, the function $\dot{m} = \dot{m}(\phi)$ that characterises

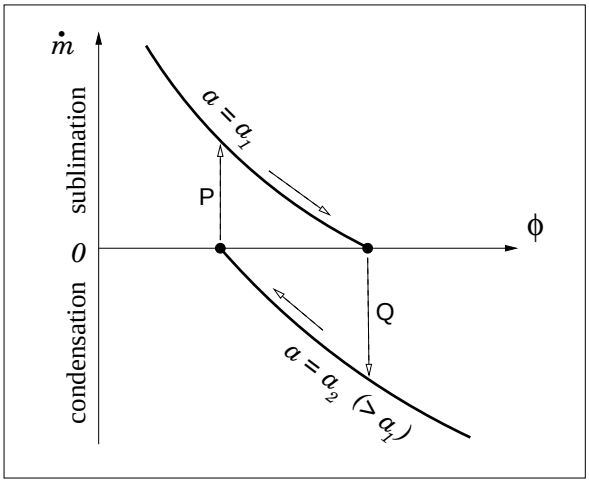

Figure 2: *Albedo-controlled oscillations in ice sublimation rate $\dot{m}$ and partial vapour pressure ϕ.*

the system at equilibrium is multi-valued, with stable branches representing high and low albedo states (Fig. 2). Essentially, a surface on which ice condenses would continue to experience condensation because its high albedo maintains a low surface temperature, keeping the atmosphere over-saturated with vapour at that temperature (Fig. 2, lower curve). Another way of stating the feedback is that T is kept below the frost point for a given ϕ. In contrast, if ice sublimates, the surface will remain dark (and above the frost point), reinforcing sublimation (Fig. 2, upper curve).

The two states do not last indefinitely. Owing to vapour depletion or enrichment, the atmosphere evolves towards saturation (with diminishing $\dot{m}$), at which point each state becomes unstable and switches into the other (described by Eqn. (3)), leading to an oscillatory cycle (Fig. 2, dashed arrows). In the presence of wind, an air packet will undergo the same transitions as it moves along the surface to produce light and dark regions, which we liken to the smooth terrain and troughs/ scarps, respectively. Due to the alternating accumulation and ablation in these regions, an undulating topography will develop that migrates and self-organises (via slope control on I_n). If u is the windspeed and x is distance downwind, mass conservation for an ideal-gas atmosphere of effective height h would imply $u d\phi/dx \approx kT\dot{m}/(hM_w)$, so that a length-scale for the spacing between troughs is $x \sim uh\phi M_w/(kT\dot{m})$. For the north polar cap and with H_2O, we obtain $h \sim 10$ to 10^3 m if (as observed) $x \sim 50$ km. (The large uncertainty arises from the poorly-known constant D; see [8]). Similar mechanisms known as Belousov-Zhabotinskii reactions have been studied in the field of biological pattern formation [9].

Discussion. Although our model is simple, the proposed mechanism is robust and points to interesting comparisons with observations. (1) The distinction between two kinds of terrain in terms of topography, albedo, and accumulation–ablation regime supports a bistable mechanism. (2) The model-predicted trough axes align in a normal direction to wind transport, such that, under a radial wind pattern modified by the Coriolis effect at both poles, large-scale spiraling of the troughs in the observed orientation would occur (anti-clockwise going out in the north, clockwise in the south). (3) The model can simulate the small width ratio of the troughs vs. smooth terrain, because the atmospheric flow attains saturation over short distances on warm, sun-facing scarps. (4) If, contrary to what is often assumed [10], the surface winds are directed *poleward*, the simulated topography would best fit the observed. This is because high ablation occurs at the base of scarps where vapour-depleted air first encounters the troughs (corresponding to transition P, Fig. 2), and high accumulation occurs atop scarps where vapour-laden air encounters smooth terrains (Q, Fig. 2). With this mass balance configuration, our model is consistent also with the stratigraphy of layered ice deduced by [1]. It can explain the extension of 'layered terrain' over the bottom of troughs, and the irregular edges of the 'banded terrain' (which mark the place where moisture can no longer condense out of the air, sensitive to atmospheric fluctuations).

Regarding the last point above, although the notion of winds flowing up the ice caps seems counter-intuitive, evidence from MOLA-detected cloud features (see [11], Figs. 9A,B) indicates that such conditions happen at least some of the time in the north. To further our study, we have begun incorporating a more detailed atmosphere, as well as the effects of seasonal and long-term cycles of wind and volatile transport, into our model simulations.

References. [1] A. D. Howard et al., *Icarus*, **50**, 161, 1982. [2] J. A. Cutts & B. H. Lewis, *Icarus*, **50**, 216, 1982. [3] J. Laskar et al., *Nature*, **419**, 375, 2002. [4] A. D. Howard, *Icarus*, **34**, 581, 1978. [5] D. A. Fisher, *Icarus*, **105**, 501, 1993. [6] D. A. Fisher, *Icarus*, **144**, 289, 2000. [7] C. S. Hvidberg, *Ann. Glaciology*, **37**, 2003 (in press). [8] A. B. Ivanov & D. O. Muhleman, *Icarus*, **144**, 436, 2000. [9] J. D. Murray, *Mathematical Biology. I: An Introduction* (3rd ed.), Springer-Verlag, 2002. [10] A. D. Howard, *Icarus*, **144**, 267, 2000. [11] M. T. Zuber et al., *Science*, **282**, 2053 ,1998.